

A Fast Piezo Actuated Tip/Tilt Mirror for raster scan applications

E. Csencsics, B. Sitz, G. Schitter

Christian Doppler Laboratory for Precision Engineering for Automated In-line Metrology, Automation and Control Institute (ACIN), Vienna University of Technology, 1040 Vienna, Austria (e-mail: csencsics@acin.tuwien.ac.at).

Abstract: This paper presents the system and control design of a novel high performance piezo-actuated fast steering mirror (FSM) for high speed optical scanning which is centered around an easy-to-manufacture membrane-like mechanical flexure and uses an optical sensor system for position measurement. With the membrane flexure the first fundamental resonance mode of the actuator is placed as high as 6.7 kHz, while still enabling an optical angular range of ± 4.8 mrad. Using a PI controller together with three notch filters designed in a loop shaping approach for maximizing the system bandwidth and tracking of high resolution raster trajectories, a closed-loop bandwidth as high as 2.7 kHz and a positioning uncertainty of 3.8 μ rad rms is obtained. The obtained tracking error when tracking a 250 Hz raster scanning trajectory with a scan amplitude of 2.2 mrad is as small as 73.8 μ rad rms (3.6% of scan amplitude).

Keywords: Fast steering mirror, System analysis and design, Motion control, Piezo actuation, Optomechanics

1. INTRODUCTION

Fast steering mirror (FSM) systems [Hedding and Lewis (1990)], also termed tip/tilt mirrors, are opto-mechatronic devices that enable tip and tilt motion of a mirror for optical pointing and scanning applications in various scientific and commercial systems. Applications for pointing operations include beam stabilization in optical systems [Kluk et al. (2012)], tracking of objects and acquisition of optical signals [Guelman et al. (2004)], image stabilization in stare imaging systems [Sun et al. (2015)] and adaptive optics in telescopes [Janssen et al. (2010)]. Applications requiring good scanning properties range from scanning laser sensors [Schlarp et al. (2018)] over scanning optical lithography [Zhou Q., et al. (2008)] to confocal microscopy [Yoo et al. (2014)] and material processing [Hedding and Lewis (1990)].

FSMs are most commonly actuated by either using piezo-electric [Tapos et al. (2005)] or voice coil actuators [Csencsics and Schitter (2017)], and more recently by reluctance actuators, which are rather rare due to their comparably large size [Csencsics et al. (2018)]. Voice coil actuators are used for systems which require a large scan range and a moderate bandwidth, such as ± 87 mrad and 350 Hz [Xiang et al. (2009)], and which are typically larger in size. Piezo-based FSMs take advantage of the small actuator size and result in comparably compact systems that enable a higher bandwidth and scan speed at a rather small scan range, such that they appear suited for the integration in high speed scanning systems [LeLetty et al. (2004)]. To obtain the required levels of precision, FSM systems, independent of the actuation principle and the application class, are most commonly controlled by feedback controllers en-

abling a high control bandwidth for good tracking and disturbance rejection performance [Kluk et al. (2012)]. Piezo actuated FSMs and other high stiffness systems, such as AFMs [Schitter et al. (2007)], are usually controlled by PI controllers, which place the crossover frequency of the loop gain below the first fundamental resonance mode of the actuator and are well suited for tracking conventionally used raster trajectories [Csencsics et al. (2016)]. Their control bandwidth is thereby typically limited by the first or second mechanical resonance of the system [Ito and Schitter (2016)].

Various piezo actuated FSMs are reported in literature with typical values for angular range and main resonance mode, of e.g. ± 1 mrad and 3 kHz [Mokbel et al. (2012)] or ± 1.6 mrad and 5.3 kHz [Park et al. (2012)]. Recent research efforts were focused on extending the range of piezo actuated FSMs up to ± 7 mrad [Shao et al. (2018)] or even ± 17.5 mrad [Wei et al. (2014)] by employing sophisticated mechanical amplification structures and flexures. These range extensions however come on the cost of the first resonance modes occurring significantly lower than 1 kHz [Shao et al. (2018); Wei et al. (2014)] which reduces the achievable closed-loop bandwidth and thus the scan speed. Key components, commonly highlighted in reported piezo FSM systems, are the rather complex flexures for suspending the mover and pre-stressing the actuators as well as the employed amplification structures. They typically require a considerable design effort, are most commonly EDM cut and in general rather challenging to optimize and manufacture [Jing et al. (2015)].

This paper presents the system and control design of a novel high performance piezo-actuated FSM system with piezo actuators in a push-pull configuration [Mokbel et al.

(2012)], which is centered around an easy-to-manufacture membrane-like flexure to ease the mechanical design challenges, and features an optical sensor system for position measurement. It investigates the resulting system performance when the FSM is operated with a feedback position controller as well as the error when it is tracking a designed high speed raster scanning trajectory. Section 2 describes the system design and elaborates on the various system components and design choices. The system identification is shown in Section 3, followed by the model-based controller design in Section 4. Section 5 evaluates the system performance along a classical raster scan case. Section 6 concludes the paper.

2. FSM SYSTEM DESIGN

2.1 System Overview

The proposed FSM system relies on two pairs of piezo stack actuators in push-pull configuration that are aligned along the two system axes and actuate the mover in tip and tilt direction. An overview of the proposed FSM system design is shown in Fig. 1. A suspension membrane is mounted to the top of the system body, suspending the mover and carrying a mirror on its top side. This membrane also provides the preloading of the piezos, which is required for dynamic operation. The actuators are mounted to a piezo mounting plate and are pushing against the backside of the mover at specific contact points. A reflective element is mounted on the backside of the mover to reflect a laser beam of the optical sensor system, which enters the system through the base plate and propagates through the center of the cylindrical system. The reflected beam hits a PSD that measures the position of the laser spot in two dimensions.

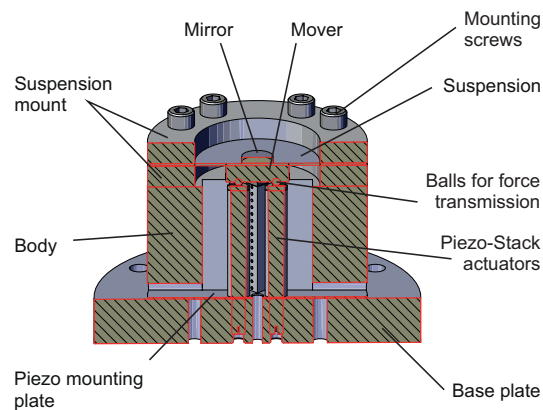


Fig. 1. Cross section view of the piezo FSM showing the system components. The mirror and the mover are attached to the suspending flexure membrane and are actuated with two stack actuators per axis.

The mover, which is a solid $\varnothing 5.5 \times 20$ mm aluminum cylinder, is designed to ensure sufficient stiffness of the moving part in order to shift structural modes to high frequencies and avoid deformations of the mirror surface during dynamic operation. To provide a force interface

from each actuator to the rotary mover that is not able to transmit tensile and shear forces, steel balls are bonded to the bottom of the mover providing a single contact point to the steel plates that are bonded to the top of each piezo actuator enabling the intended rotational motion of the mover.

For actuation four PICMA stack actuators (Model P-885.91, Physik Instrumente GmbH & Co. KG, Germany) with a length of 36 mm (max. displacement $38 \mu\text{m}$) are used and placed in a distance of 6 mm from the system center. Each actuator pair is operated in a push-pull configuration to obtain a pure rotational motion of the mover. In the zero position the actuators are already elongated by half their range, in order to enable bi-directional motion of each actuator [Schitter et al. (2007)] and thus bi-directional rotational movement of the mirror around the zero position. This denotes that at the maximum rotational displacement, one actuator has its minimal, while the other actuator has its maximum elongation. As the piezo actuators can not be used to exert pulling forces on the mover, they have to be pre-stressed in order to maintain contact to the mover when retracting and thus enable dynamic operation. The actuators are bonded to a thin piezo mounting plate (cf. Fig. 1), which is attached to the base plate. This mounting plate restricts lateral movement but enables individual vertical adjustment of the stack actuator to fine align them to the flexure by means of set screws in the base plate.

2.2 Suspension System

The suspension system is designed as a metallic membrane which carries the mirror and the mover centrally bonded to its front and backside, respectively. It is clamped onto the body of FSM system with two mounting rings, connecting the static and moving part of the system. It is further used for pre-stressing the piezo actuators for dynamic operation. When increasing the stiffness of the flexure (by making it thicker), the range of the actuators in the pre-stressed case is reduced accordingly [Munnig-Schmidt et al. (2014)]

$$\Delta L_A \approx L_0 \left(1 - \frac{k_A}{k_A + k_S} \right) \quad (1)$$

with k_A the stiffness of the actuator, k_S the stiffness of the flexure, and L_0 being the range of the stack actuator in the stress-free case. Making the flexure stiffer on the other hand also increases the frequencies of its structural modes, which is beneficial from a controls perspective. This results in two competing design aspects: (i) the flexure needs to be sufficiently stiff to push the main resonance mode to a high high frequency and (ii) it needs to be compliant enough to not significantly reduce the range of the piezo stacks.

After evaluating several membrane-material-configurations on the basis of a static mechanical finite element analysis performed in ANSYS (Ansys Inc., PA, USA) a 0.8 mm brass flexure is chosen for the FSM design, as it provides a good trade-off between range loss and main resonance mode. A modal analysis is used throughout the flexure design to obtain the structural modes of the flexure. The designed flexure shows a piston mode at 3.8 kHz, the

desired tilt mode at 6.5 kHz, which is depicted in Fig. 2, and a first higher structural mode at 28.4 kHz.

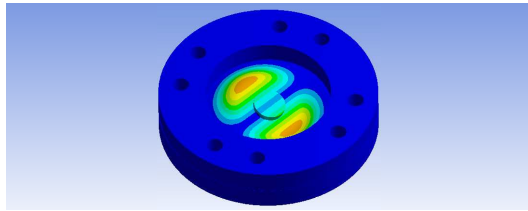


Fig. 2. Modal analysis of the flexure membrane. The tilt mode of the flexure occurs at 6.5 kHz.

2.3 System Setup

The entire experimental system setup is depicted in Fig. 3a, showing the FSM system with the mirror mount and the components of the optical sensor system, including the custom made readout electronics. The optical sensor system is located behind the mirror unit and comprises a laser source, a beam splitter and a position sensitive device (PSD; S5990-01, Hamamatsu Photonics, Japan) for detecting displacements of the reflected laser spot in x- and y-direction. A front view of the system with the 10 mm mirror bonded to the flexure membrane is shown in Fig. 3b, while Fig. 3c depicts the backside of the flexure with the mounted mover, the steel balls and the sensor mirror for the optical sensor system, which reflects the incoming laser beam. The piezo actuators are operated in a push-pull configuration and are driven by a piezo amplifier (Techproject EMC GmbH, Austria; output voltage 0-150V) with a measured bandwidth of 10 kHz and a second order lowpass characteristic at higher frequencies. The comparably low amplifier bandwidth is chosen deliberately as it can be directly employed to significantly reduce the excitation of higher modes of the mechanical system. For deriving input signals for the amplifier, acquiring the position signals, and controller implementation a real-time data acquisition system (Type: DS1202, dSPACE GmbH, Germany) is used. The optical sensor system is calibrated by using an external reference metrology system (Confocal sensor confocalDT 2451, Micro-Epsilon Messtechnik GmbH & Co. KG, Germany), which measures the mirror position from the front side and uses a small angle approximation to obtain the angular displacement.

3. SYSTEM IDENTIFICATION

For identifying the dynamics of the FSM prototype system a system analyzer (3562A, Hewlett-Packard, Palo Alto, CA, USA) is used. The inputs of the piezo amplifier and the output signals of the optical sensor system are considered as system inputs and outputs, respectively.

Figure 4 shows the measured frequency response data of the x- (blue) and y-axis (red) of the system. It can be seen that both system axes show almost identical dynamics, with only slight deviations resulting most likely from mounting tolerances. The main resonance mode occurs at 6.7 kHz and shows good agreement with the predicted value from the flexure design in Section 2.2. Below this

mode two more modes at 3 kHz and 3.6 kHz can be observed. The mode at 3.6 kHz can be matched to the piston mode of the modal analysis, which might be excited due to unsynchronized piezo motion caused by hysteresis or imperfect alignment. The mode at 3 kHz does not appear in the modal analysis but may be explained by the finite stiffness of the upright supporting structure Schitter et al. (2007). Above the main resonance mode the system shows fourth order lowpass characteristics, which reduces the excitation of higher system modes and is due to the piezo amplifier bandwidth. For modeling the measured frequency responses of both axes an 8th order plant model

$$G(s) = K \cdot \frac{\left(\prod_{i=1}^2 s^2 + 2\zeta_{z_i}\omega_{z_i}s + \omega_{z_i}^2 \right)}{\left(\prod_{i=1}^4 s^2 + 2\zeta_{p_i}\omega_{p_i}s + \omega_{p_i}^2 \right)} \cdot e^{-sT}, \quad (2)$$

with gain $K = 5.82e16$, time delay $T = 16.7 \mu s$ (sampling delay of the dSpace system), and parameters according to Table 1 is obtained. Crosstalk measurements (data not

Table 1. Coefficients of the FSM system model $G(s)$.

Index	ω_{Index} [rad/s]	ζ_{Index}
z_1	2.05e4	0.03
z_2	2.41e4	0.02
p_1	1.93e4	0.05
p_2	2.29e4	0.02
p_3	4.26e4	0.05
p_4	5.03e4	0.44

shown) revealed that the crosstalk between the axes at DC is more than 30 dB smaller than the magnitudes of the individual system axes, which justifies the application of one single-input-single-output (SISO) feedback controller per axis.

The mechanical system range and hysteresis of the stack actuators are measured by applying a 1 Hz sinusoidal signal with 10 V amplitude to the piezo amplifier input of one system axis at a time. The measurement results (data not shown) reveal a mechanical range of ± 2.4 mrad (± 4.8 mrad optical) in tip and tilt direction, as well as a maximum hysteresis of about 15% for both system axes.

4. CONTROLLER DESIGN

The design of the feedback controller is done with the aim of maximizing the closed-loop system bandwidth for high speed scanning operation.

4.1 PI Controller with Notch Filters (PI+ Controller)

As most commercial piezo actuated FSM systems use feedback bandwidth controllers for position control of the mirror, a PI based controller design is taken as starting point for both axes. PI controllers with a crossover frequency below the first fundamental resonance mode of the actuator are also applied in many other piezo actuated high stiffness systems, such as AFMs [Schitter et al. (2007)], for tracking raster trajectories with their various frequency components [Fleming and Wills (2009)]. The P-gain is used to vertically shift the loop gain and adds artificial stiffness

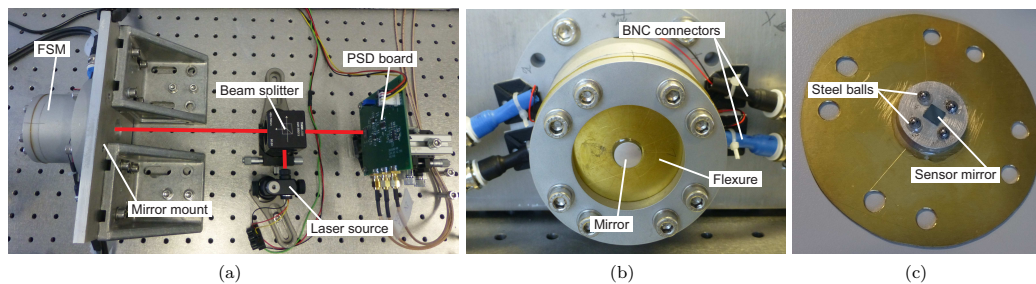


Fig. 3. Experimental FSM system setup. (a) depicts an overview of the entire setup with the FSM, its mounting plate and the optical position sensor system with laser source, beam splitter and PSD board. (b) shows a front view of the FSM, with the mirror, the flexure membrane and the BNC connectors for the actuators observable. (c) shows the backside of the mover with the mounted mover, the steel balls and the sensor mirror.

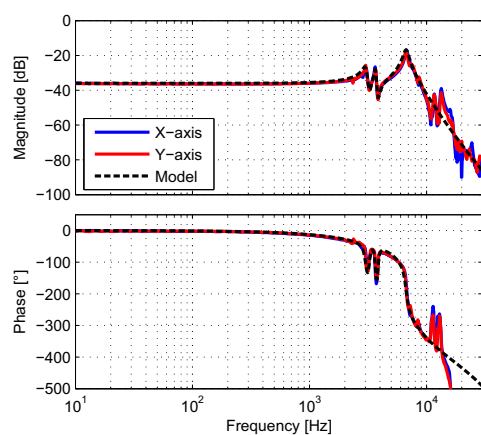


Fig. 4. Frequency response of the FSM x- (solid blue) and y-axis (solid red) measured with the optical sensor system. The fitted system model (dashed black) models the first three system resonances at 3, 3.6 and 6.7 kHz.

to the system. The integrator increases the loop gain at low frequencies, enforcing high tracking performance and zero steady state error. Looking at the mode at 6.7 kHz and its peak value of -16.9 dB the achievable crossover frequency would be limited to about 75 Hz when using solely a PI controller. To extend the bandwidth three tuned notch filters [Munnig-Schmidt et al. (2014)] (also see Fig. 5) of the form

$$N(s) = \frac{s^2 + 2d_n w_n \omega_n s + \omega_n^2}{s^2 + 2w_n \omega_n s + \omega_n^2}, \quad (3)$$

with d_n the depth, w_n the width of the notch and ω_n the frequency at which the notch is placed, are designed and added to the controller to cancel the first three resonance peaks identified in Section 3. In a loop shaping approach, aiming to maximize the system bandwidth, the PI+ controller

$$C(s) = K \cdot \frac{\left(\prod_{i=1}^3 s^2 + 2d_n w_n \omega_n s + \omega_n^2 \right) \cdot (s + \omega_4)}{\left(\prod_{i=1}^3 s^2 + 2w_n \omega_n s + \omega_n^2 \right) s} \quad (4)$$

with $K = 50$ and parameters according to Table 2, is designed for a crossover frequency of 1.4 kHz. The

Table 2. Coefficients of the designed PI+ controller.

Index	ω_{Index} [rad/s]	d_{Index}	w_{Index}
1	1.94e4	0.5	0.2
2	2.29e4	0.5	0.1
3	4.26e4	0.025	2
4	1e4	-	-

simulated open loop response of the designed controller and the derived plant model shows a gain margin of 6.4 dB and a phase margin of 63°. The simulated closed-loop bandwidth is 3 kHz. As the dynamics of both system axes are similar, the same controller can be applied to both system axes.

4.2 Controller Implementation

For implementation on the dSpace system the controllers are discretized using Pole-Zero-Matching for a sampling frequency of $f_s = 60$ kHz [Franklin et al. (1997)]. The poles and zeros are directly transformed to the discrete time domain by using the relation $z = e^{s/f_s}$ to guarantee that the notch filter are located exactly at the desired frequencies.

Fig. 5 shows the frequency responses of the implemented PI+ controller together with the frequency responses of its PI and notch filter components. The PI component (dashed blue) shows integrating behavior at low frequencies and constant gain at high frequencies. The first two notch filters $N_1(s)$ and $N_2(s)$ (dotted and dashed black) have the same depth value $d_1 = d_2 = 0.5$ ($w_1 = 0.2$, $w_2 = 0.1$), are located at 3 and 3.6 kHz, respectively, and are used to cancel the two small resonance peaks at these frequencies. The third notch filter $N_3(s)$ (dash-dotted black) is placed at 6.7 kHz and is significantly deeper and wider ($d_3 = 0.025$, $w_3 = 2$) in order to notch out the main resonance mode of the FSM dynamics. The

resulting transfer function of all notch filters $N_g(s)$ (dashed cyan) is also shown.

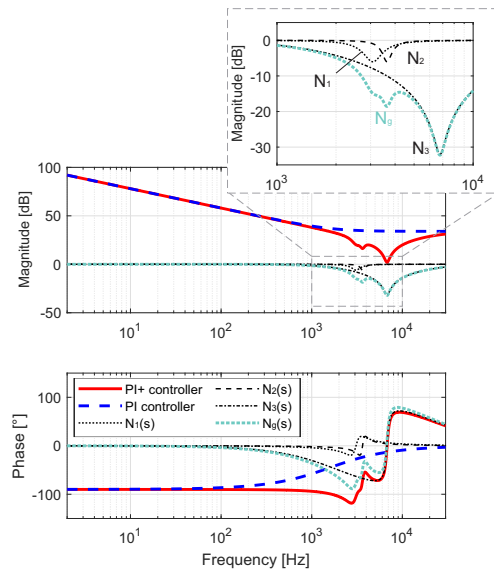


Fig. 5. Measured frequency response of the implemented PI+ controller (solid red). It is designed for a crossover frequency of 1.4 kHz, comprising a PI component (dashed blue), as well as notch filters (black) at 3 ($N_1(s)$), 3.6 ($N_2(s)$) and 6.7 kHz ($N_3(s)$).

5. EVALUATION OF SYSTEM PERFORMANCE

For evaluation of the system performance, the closed-loop system dynamics, the tracking performance, and the positioning uncertainty are investigated. For testing the tracking performance a raster trajectory with high spatial and temporal resolution, which has its first 11 harmonics covered by the closed-loop bandwidth, is obtained by selecting $f_{1R} = 250$ Hz and $f_{2R} = 0.5$ Hz for the fast and slow scan axis, respectively. The resulting spatial resolution is $4 \mu\text{rad}/\text{mrad}$ at a frame rate of 1 frame/s.

The measured complementary sensitivity function of the FSM system with the PI+ controller is shown in Fig. 6, together with the modeled closed-loop system dynamics. The measured frequency response shows good agreement with the modeled response. The resulting system bandwidth 2.7 kHz matches well with the 3 kHz predicted by the model. The measured dynamics show a small gain peaking of 2.5 dB at 1.9 kHz, which is due to the relatively large phase margin.

To evaluate the tracking performance of the closed-loop system, the designed raster trajectory is applied with a scan amplitude of 2.2 mrad and tracked with the PI+ controllers. The measured signals are post-processed by low-pass filters with a bandwidth of 20 kHz for reducing high frequency noise. The results of the fast scan axis are depicted in Fig. 7. The tracking error for the entire trajectory results to $73.8 \mu\text{rad}$ rms (3.6% of the scan

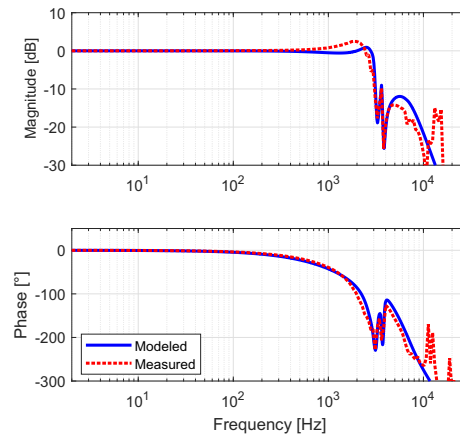


Fig. 6. Modeled (solid blue) and measured (dashed red) complementary sensitivity function of the FSM with the PI+ controller. The measured dynamics shows a control bandwidth of 2.7 kHz.

amplitude) and 0.61 mrad peak-to-valley error, with a controller output of 71.9 V rms. Disregarding the data around the turning points of the fast axis (80% threshold; see Fig. 7) where the tracking error is largest, the tracking error in the region of interest results to $41.4 \mu\text{rad}$ rms (1.9% of the scan amplitude) and 0.48 mrad peak-to-valley. The resulting positioning uncertainty of the FSM system controlled by the PI+ controller is determined at zero reference applied to both axes and is as small as $3.8 \mu\text{rad}$ rms, which is 0.08% of the full scale range.

In summary it is successfully demonstrated that the proposed piezo actuated FSM with the novel membrane flexure, optical position sensor system and ± 2.4 mrad mechanical angular range achieves a closed-loop bandwidth of 2.7 kHz with the PI+ controller, and shows good tracking performance as well as a low positioning uncertainty.

6. CONCLUSION

This paper presents a novel piezo-actuated FSM system design with an optical position sensor system for high speed scanning applications. The design is centered around an easy-to-manufacture membrane-like metallic flexure and two pairs of stack actuators that are operated in a push-pull configuration. It provides a mechanical angular range of ± 2.4 mrad (± 4.8 mrad optically) in both axes, while achieving a first fundamental resonance mode of the actuator as high as 6.7 kHz. After a detailed system description and analysis, a model-based PI+ controller for maximizing the system bandwidth and tracking of raster trajectories is designed. The resulting closed-loop system has a bandwidth as high as 2.7 kHz and a small positioning uncertainty of $3.8 \mu\text{rad}$ rms.

ACKNOWLEDGEMENTS

The financial support by the Christian Doppler Research Association, the Austrian Federal Ministry for Digital and

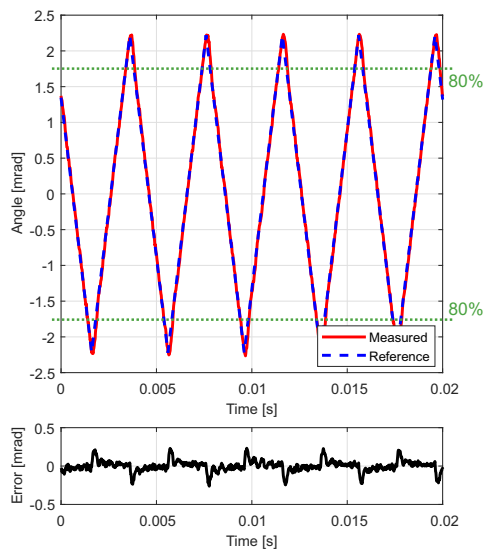


Fig. 7. Measured raster scan trajectory. The reference (dashed blue), the measured position signal (solid red) and the tracking error (solid black) of the fast scan axis tracking a 250 Hz triangular signal are shown.

Economic Affairs, and the National Foundation for Research, Technology and Development, as well as MICRO-EPSILON MESSTECHNIK GmbH & Co. KG and ATENSOR Engineering and Technology Systems GmbH is gratefully acknowledged.

REFERENCES

- Csencsics, E., Saathof, R., and Schitter, G. (2016). Design of a dual-tone controller for lissajous-based scanning of fast steering mirrors. *American Control Conference, Boston, MA, USA*.
- Csencsics, E. and Schitter, G. (2017). System design and control of a resonant fast steering mirror for lissajous-based scanning. *IEEE TMECH*, 22(5), 1963–1972.
- Csencsics, E., Schlarp, J., and Schitter, G. (2018). High-performance hybrid-reluctance-force-based tip/tilt system: Design, control, and evaluation. *IEEE TMECH*, 23(5), 2494–2502.
- Fleming, A.J. and Wills, A.G. (2009). Optimal periodic trajectories for band limited systems. *IEEE TCST*, 17(3), 552–562.
- Franklin, G.F., Powell, D.J., and Workman, M.L. (1997). *Digital Control of Dynamic Systems*. Prentice Hall.
- Guelman, M., Kogan, A., Livne, A., Orenstein, M., and Michalik, H. (2004). Acquisition and pointing control for inter-satellite laser communications. *IEEE Transactions on Aerospace and Electronic Systems*, 40(4), 1239.
- Hedding, L.R. and Lewis, R.A. (1990). Fast steering mirror design and performance for stabilization and single axis scanning. *SPIE 340*, 1304, 14–24.
- Ito, S. and Schitter, G. (2016). Comparison and classification of high-precision actuators based on stiffness influencing vibration isolation. *IEEE TMECH*, 21(2), 1169–1179.
- Janssen, H., Teuwen, M., Navarro, R., Tromp, N., Elswijk, E., and Hanenburg, H. (2010). Design and prototype performance of an innovative cryogenic tip-tilt mirror. *Modern Technologies in Space and Ground-based Telescopes, Proceedings of the SPIE*, 77394A.
- Jing, Z., Xu, M., and Feng, B. (2015). Modeling and optimization of a novel twoaxis mirror-scanning mechanism driven by piezoelectric actuators. *Smart Materials and Structures*, 24(2), 025002.
- Kluk, D.J., Boulet, M.T., and Trumper, D.L. (2012). A high-bandwidth, high-precision, two-axis steering mirror with moving iron actuator. *Mechatronics*, 22(3), 257.
- LeLetty, R., Barillot, F., Fabbro, H., Claeysen, F., Guay, P., and Cadiergues, L. (2004). Miniature piezo mechanisms for optical and space applications. *9th International Conference on New Actuators, Germany*.
- Mokbel, H.F., Yuan, W., Ying, L.Q., Hua, C.G., and Roshdy, A.A. (2012). Research on the mechanical design of two-axis fast steering mirror for optical beam guidance. *International Conference on Mechanical Engineering and Material Science*.
- Munnig-Schmidt, R., Schitter, G., Rankers, A., and van Eijk, J. (2014). *The Design of High Performance Mechatronics*. Delft University Press, 2nd edition.
- Park, J.H., Lee, H.S., Lee, J.H., Yun, S.N., Ham, Y.B., and Yun, D.W. (2012). Design of a piezoelectric-driven tilt mirror for a fast laser scanner. *Japanese Journal of Applied Physics*, 51(9S2), 09MD14.
- Schitter, G., Astrom, K.J., DeMartini, B.E., Thurner, P.J., Turner, K.L., and Hansma, P.K. (2007). Design and modeling of a high-speed afm-scanner. *IEEE TCST*, 15(5), 906–915.
- Schlarp, J., Csencsics, E., and Schitter, G. (2018). Optical scanning of laser line sensors for 3d imaging. *Applied Optics*, 57(18), 5242–5248.
- Shao, S., Tian, Z., Song, S., and Xu, M. (2018). Two-degrees-of-freedom piezo-driven fast steering mirror with cross-axis decoupling capability. *Review of Scientific Instruments*, 89(5), 055003.
- Sun, C., Ding, Y., Wang, D., and Tian, D. (2015). Backscanning step and stare imaging system with high frame rate and wide coverage. *Applied Optics*, 54(16), 4960–4965.
- Tapos, F.M., Edinger, D.J., Hilby, T.R., Ni, M.S., Holmes, B.C., and Stubbs, D.M. (2005). High bandwidth fast steering mirror. *Proceedings of SPIE*, 5877.
- Wei, C., Sihai, C., Xin, W., and Dong, L. (2014). A new two-dimensional fast steering mirror based on piezoelectric actuators. *4th IEEE International Conference on Information Science and Technology*, 308–311.
- Xiang, S., Wang, P., Chen, S., Wu, X., Xiao, D., and Zheng, X. (2009). The research of a novel single mirror 2d laser scanner. *Proc. of SPIE*, 7382.
- Yoo, H., van Royen, M.E., van Cappellen, W.A., Houtsmuller, A.B., Verhaegen, M., and Schitter, G. (2014). Automated spherical aberration correction in scanning confocal microscopy. *Review of Scientific Instruments*, 85, 123706.
- Zhou Q., et al. (2008). Design of fast and steering mirror and systems for precision and laser beams and steering. *IEEE Workshop on Robotic and Sensors Environments*.